k-inflation: Non-separable case meets ACT measurements

Tahere Fallahi Serish,[1,*] Seyed Ali Hosseini Mansoori,[1,†] Fereshteh Felegary,[2,‡] Özgür Akarsu,[3,§] M. Sami[4,5,¶]

[1] *Faculty of Physics, Shahrood University of Technology, P.O. Box 3619995161 Shahrood, Iran*
[2] *School of Astronomy, Institute for Research in Fundamental Sciences (IPM), Tehran, Iran, P.O. Box 19395-5531*
[3] *Department of Physics, Istanbul Technical University, Maslak 34469 Istanbul, Türkiye*
[4] *Centre for Cosmology and Science Popularization (CCSP), SGT University, Gurugram, Delhi- NCR, Haryana- 122505, India*
[5] *Eurasian International Centre for Theoretical Physics, Astana, Kazakhstan*

We investigate a non-separable subset of k-essence in which the kinetic and potential sectors interact through an $X^\rho V(\phi)$ coupling, implemented via a potential-dependent prefactor $f(\phi) = 1 + 2\mathcal{K}V$. In slow roll, this structure preserves a constant sound speed $c_s^2 = 1/(2\rho - 1)$ while modifying the Hubble flow in a controlled way, thereby shifting the inflationary observables relative to the separable template. For monomial potentials $V = A\phi^n$ (with $n = 2$ and $n = 2/3$ as representative cases) we derive closed analytic expressions for $n_s(N_*)$ and $r(N_*)$ to $\mathcal{O}(\epsilon^2_{\rm mix})$, where $\epsilon_{\rm mix} \propto \mathcal{K}$ encodes the non-separable $X^\rho V$ mixing, and we validate them against exact background integrations. The analytic and numerical predictions agree at the sub-per-mille level for n_s and at the percent level for r, confirming the accuracy of the small-mixing expansion. For $\mathcal{K} < 0$ the mixing systematically lowers both n_s and r at fixed N_*, allowing otherwise marginal monomials to fall within the region favored by recent ACT+*Planck*+BAO constraints (P–ACT–LB). All solutions shown satisfy the health conditions $f(\phi) > 0$, $\rho > \frac{1}{2}$, and the positivity bound $V < 1/(2|\mathcal{K}|)$ (from $f > 0$). We also discuss parameter dependence and the expected equilateral-type non-Gaussianity, which remains comfortably within current bounds for the benchmarks considered.

I. INTRODUCTION

Inflation provides a compelling mechanism to resolve the horizon, flatness, and monopole problems of standard big–bang cosmology while generating the primordial fluctuations that seed large–scale structure [1–5]. Quantum fluctuations of the inflaton field source metric perturbations, whose imprints on the cosmic microwave background (CMB) are captured, to leading order, by two key observables: the scalar spectral index n_s, encoding the scale dependence of curvature perturbations, and the tensor–to–scalar ratio r, measuring the relative amplitude of primordial gravitational waves.

Over the past decades, successive space and ground experiments—from COBE and WMAP [6] to Planck [7], ACT [8, 9], and SPT [10]—have progressively sharpened these constraints. The Planck–only value $n_s = 0.9649 \pm 0.0042$ [7] is shifted upward in joint ACT+Planck analyses (P–ACT), which find $n_s = 0.9709 \pm 0.0038$; including BAO/DESI information (P–ACT–LB) further yields $n_s = 0.9743 \pm 0.0034$ together with $r < 0.038$ (95% CL) [8, 9]. For comparison, the current SPT/Planck combination gives $n_s = 0.9647 \pm 0.0037$ [10]. The upward shift in n_s is phenomenologically significant: it places pressure on a number of otherwise successful benchmarks and has motivated a broad set of refinements and alternatives, including deformations of Starobinsky/attractor realizations, non/minimally coupled models, and higher–curvature frameworks [11–48].

Within single–field scenarios, k-inflation [49] (or, more broadly, k–essence) retains minimal coupling to gravity while generalizing the Lagrangian to $P(X, \phi)$, with $X \equiv -\partial_\mu\phi\,\partial^\mu\phi/2$. This framework admits a subluminal sound speed $c_s \leq 1$ and, in general, distinctive non–Gaussian signatures. Most phenomenological applications adopt a sum–separable structure, $P(X) + U(\phi)$. In this work we explore a simple non-separable template where the kinetic and potential sectors interact multiplicatively via an $X^\rho V(\phi)$ coupling, encoded by $P(X, \phi) = f(\phi)\,[X^\rho - V(\phi)]$ with $f(\phi) = 1 + \frac{2\mathcal{K}}{M^4_{\rm pl}} V(\phi)$ and $\rho > \frac{1}{2}$. This structure preserves a constant sound speed $c_s^2 = 1/(2\rho - 1)$ and modifies the slow-roll Hubble flow in a controlled way, thereby shifting (n_s, r) relative to the separable template. The sign of the mixing parameter $\mathcal{K}$ is model–dependent; here we focus on $\mathcal{K} < 0$, for which $0 < f(\phi) < 1$ during slow roll and the mixing remains perturbative, while predictions tend to move toward the recent P–ACT–LB preferred region. (An EFT rationale for $f(\phi)$ and its sign is given in Sec. II.)

Our goals are twofold. First, for monomial potentials $V = A\phi^n$ (with $n = 2$ and $n = 2/3$ as representative cases), we derive closed analytic expressions for $n_s(N_*)$ and $r(N_*)$ to $\mathcal{O}(\epsilon^2_{\rm mix})$, where the small parameter $\epsilon_{\rm mix} \propto \mathcal{K}$ naturally encodes the non–separable $X^\rho V$ mixing. We validate these expressions against exact background integrations, finding excellent agreement in the small–mixing regime. Second, we map the dependence of (n_s, r) on $(N_*, \rho, \epsilon_{\rm mix})$ and compare the resulting predictions with recent ACT+Planck+BAO contours (P–ACT–LB) via parameter–space overlays in the (n_s, r) plane. This investigation clarifies the roles of N_*

* fallahi.ta@shahroodut.ac.ir
† shosseini@shahroodut.ac.ir
‡ fereshteh.felegary@gmail.com
§ akarsuo@itu.edu.tr
¶ sami_ccsp@sgtuniversity.org

(primarily setting n_s), ρ (via the constant c_s), and the mixing strength $\epsilon_{\rm mix}$ (which tunes both observables), and it highlights regimes in which otherwise marginal monomials become compatible with current bounds. In particular, we show that even for simple chaotic monomials the non–separable mixing can move predictions into the P–ACT–LB–favored region.

The paper is organized as follows. In Sec. II we introduce the setup and slow-roll background, including stability conditions and the constant sound speed. In Sec. III we derive analytic formulae for the slow-roll parameters and observables in terms of $(N_*, \rho, \epsilon_{\rm mix})$. In Sec. IV we compare these expressions with exact integrations and recent constraints, presenting representative tables and parameter–space plots. We summarize and discuss future directions in Sec. V.

II. SETUP

Among k-essence models [49, 50], we are led to consider a simple but instructive non-separable template in which the kinetic and potential sectors do not merely add but interact multiplicatively. Concretely, we take

$$P(X,\phi) = f(\phi)\big[X^\rho - V(\phi)\big], \tag{1}$$

where $X \equiv -\frac{1}{2}\,\partial_\mu\phi\,\partial^\mu\phi$ is the canonical kinetic invariant, $V(\phi)$ is the inflaton potential, and $\rho > 0$ is a constant exponent controlling the departure from canonical dynamics. The hallmark of (1) is the prefactor $f(\phi)$, which we choose to depend on the potential itself,

$$f(\phi) = 1 + \frac{2\mathcal{K}}{M_{\rm pl}^4}\,V(\phi), \tag{2}$$

with $\mathcal{K}$ a dimensionless coupling. We henceforth work in reduced Planck units, $M_{\rm pl} = 1$, so $f(\phi) = 1 + 2\mathcal{K}V$. This choice captures the lowest-order non-separable mixing between X and V in a low-energy expansion: the Lagrangian effectively contains an $X^\rho V$ interaction whose strength is modulated by $f(\phi)$. In the limit $\mathcal{K} \to 0$, the mixing switches off and (1) reduces continuously to the familiar separable, non-canonical case $P(X) + U(\phi)$ [51]. We work in reduced Planck units ($M_{\rm pl} = 1$) unless stated otherwise.

The potential dependence of f admits a natural rationale in effective field theory (EFT).[1] The sign of $\mathcal{K}$ is not dictated *a priori* by this EFT reasoning—both signs can arise depending on the UV couplings. In what follows we focus on the regime $\mathcal{K} < 0$. For positive $V(\phi)$ during slow roll, this choice keeps the prefactor in the controlled window $0 < f(\phi) < 1$ and implies the bound $V(\phi) < M_{\rm pl}^4/(2|\mathcal{K}|)$, which in our units reads $V < 1/(2|\mathcal{K}|)$. This ensures that the non-separable mixing remains perturbative, $|\mathcal{K}|V \ll 1$. Phenomenologically, this sign typically shifts the inflationary observables (n_s, r) downward relative to the separable limit for the potentials we study, improving agreement with the ACT-preferred region; quantitative comparisons are deferred to the Results.

In summary, our working hypothesis (1)–(2) provides a minimal arena in which a potential-dependent prefactor modulates non-canonical dynamics. The multiplicative structure is the key novelty—turning the sum of two sectors into an interaction—and the special case $\rho = 1$ smoothly connects to the XV model analyzed in [55]. In the next section we derive the background equations implied by (1) and track how the coupling in (2) imprints on the slow-roll evolution and, ultimately, on the spectral index n_s and the tensor-to-scalar ratio r.

III. BACKGROUND EQUATIONS AND INFLATIONARY PARAMETERS

Working in a spatially flat FLRW spacetime and reduced Planck units ($M_{\rm pl} = 1$), the background dynamics implied by (1) are governed by the Friedmann relation

$$3H^2 = f\big[V + (2\rho - 1)X^\rho\big]\,, \tag{3}$$

and by the k-essence continuity (or field) equation, which can be written as

$$\begin{aligned} &6\rho\, f\, H\, X^\rho + \rho(2\rho-1)\, f\, X^{\rho-1}\dot{X} \\ &= -\,\dot{\phi}\Big[(V + (2\rho-1)X^\rho)\, f_{,\phi} + f\, V_{,\phi}\Big]\,, \end{aligned} \tag{4}$$

where a comma and a dot denote derivatives with respect to ϕ and t, respectively, and $f_{,\phi} = 2\mathcal{K}\, V_{,\phi}$.

In the slow-roll regime we assume a potential-dominated energy budget and slowly varying kinetic energy,

$$(2\rho-1)\, X^\rho \ll V\,, \qquad \frac{|\dot{X}|}{HX} \ll 1\,, \tag{5}$$

under which the background equations simplify to

$$3H^2 \simeq f\,V\,, \tag{6}$$

$$6\rho\, H\, f\, X^\rho \simeq -\,\dot{\phi}\, V_{,\phi}\,(2f - 1)\,, \tag{7}$$

with $(2f-1) = 1 + 4\mathcal{K}V$. Since $V > 0$ during slow roll, Eq. (6) implies $f > 0$ along the trajectory.

[1] One convenient route is to start from a multi-field completion where heavy modes couple to both the inflaton potential and its kinetic sector. After integrating out the heavy degrees of freedom, the single-clock description can acquire a non-separable $P(X,\phi)$ with ϕ-dependent Wilson coefficients. Expanding those coefficients in $V/M_{\rm pl}^4$ (or, equivalently, in inverse powers of the heavy mass scale) yields $f(\phi) = 1 + c_1\, V/M_{\rm pl}^4 + \cdots$. Retaining the lowest-order correction and identifying $c_1 \equiv 2\mathcal{K}$ reproduces (2) and, with (1), generates the lowest-order $X^\rho V$ mixing beyond the separable template. See, e.g., Refs. [52–54].

Finally, stability of cosmological scalar perturbations requires $P_{,X} > 0$ and $c_s^2 > 0$ [50]. For the Lagrangian (1)–(2) one finds

$$P_{,X} = f\,\rho\,X^{\rho-1}\,, \qquad c_s^2 = \frac{P_{,X}}{P_{,X} + 2XP_{,XX}} = \frac{1}{2\rho-1}\,,$$

so the conditions reduce to $f(\phi) > 0$ and $\rho > \frac{1}{2}$, with constant sound speed ($s \equiv \dot{c}_s/(Hc_s) = 0$). In what follows we focus on $\mathcal{K} < 0$; together with $V > 0$ this implies the useful bound $V(\phi) < 1/(2|\mathcal{K}|)$, which we impose in all parameter scans.

Having established the slow-roll background, it is convenient to relate the Hubble slow-roll parameter directly to potential data. Differentiating Eq. (6) gives

$$\varepsilon_H \equiv -\frac{\dot{H}}{H^2} \simeq -\frac{1}{2}\left(\frac{V_{,\phi}}{V}\right)\left(\frac{\dot{\phi}}{H}\right)\left(\frac{2f-1}{f}\right). \tag{8}$$

Next, using the slow-roll field relation (7) together with $X = \dot{\phi}^2/2$, one solves for the velocity–Hubble ratio as

$$\frac{\dot{\phi}}{H} = -\,C_\rho\left[\frac{(2f-1)\,V_{,\phi}}{f^{\rho+1}\,V^{\rho}}\right]^{\frac{1}{2\rho-1}}, \tag{9}$$

where $C_\rho \equiv \left(\frac{6^{\,\rho-1}}{\rho}\right)^{\frac{1}{2\rho-1}}$. For $\rho = 1$ this reduces to $\dot{\phi}/H = -\,(2f-1)\,V_{,\phi}/(f^2V)$, in agreement with (7) and $3H^2 \simeq fV$. Combining (8) with (9) yields a compact expression for ε_H,

$$\varepsilon_H \simeq \frac{C_\rho}{2}\left[\frac{(2f-1)^{2\rho}\,V_{,\phi}^{2\rho}}{f^{3\rho}\,V^{3\rho-1}}\right]^{\frac{1}{2\rho-1}}, \tag{10}$$

while the exact relation in this model is $\varepsilon_H = \frac{3\rho\,X^{\rho}}{V+(2\rho-1)X^{\rho}}$, which reduces to $\varepsilon_H \simeq 3\rho X^{\rho}/V$ under the slow-roll conditions stated above.

During inflation the Hubble slow-roll parameters must remain small, $\varepsilon_H \ll 1$ and $\eta_H \equiv \dot{\varepsilon}_H/(H\,\varepsilon_H) \ll 1$, for roughly 50–60 e-folds to solve the flatness and horizon problems. Inflation ends when ε_H approaches unity; more generally, it is sufficient that either ε_H or $|\eta_H|$ becomes $\mathcal{O}(1)$.

Additionally, the number of e-folds, N, measures the total inflation elapsed by its end (from a given field value to the end of inflation) and is

$$N = \int_t^{t_e} H\,dt = \int_V^{V_e} \frac{1}{2\,\varepsilon_H}\,\frac{2f-1}{f}\,\frac{dV}{V}\,, \tag{11}$$

where we used Eq. (8) together with $dN = -\,H\,dt = -\,d\phi/(\dot{\phi}/H)$ and the change of variables $d\phi = dV/V_{,\phi}$. We adopt the remaining–e–folds convention $N(t) = \int_t^{t_e} H\,dt$, so N decreases to 0 at t_e. Here and below, the subscript e denotes evaluation at the end of inflation.

For concreteness we take a monomial potential

$$V(\phi) = A\,\phi^n, \tag{12}$$

with n a rational number and A a normalization fixed by the scalar power spectrum at the CMB pivot $k_* = 0.05\,\mathrm{Mpc}^{-1}$, $\mathcal{P}_* \simeq 2.1\times10^{-9}$. We denote by N_* the value of the remaining e-folds N when the pivot mode exits the sound-horizon, i.e., at $c_s k_* = aH$. Using (9) with $C_\rho \equiv (6^{\rho-1}/\rho)^{1/(2\rho-1)}$ and $c_s^2 = 1/(2\rho-1)$, Eq. (11) can be integrated in closed form:

$$N = \frac{c_s^2\left(\frac{V}{A}\right)^{\frac{\rho c_s^2}{n}} V^{c_s^2(\rho-1)}}{n^{c_s^2}\,C_\rho\,\mathcal{I}_{11}(\rho,n)\,\mathcal{I}_{32}(\rho,n)}\left[\frac{\mathcal{I}_{32}(\rho,n)}{c_s^2}\,F_1\!\left(\frac{\mathcal{I}_{11}(\rho,n)}{n}, -c_s^2(1+\rho), 2\rho c_s^2; \frac{\mathcal{I}_{32}(\rho,n)}{n}; -2\mathcal{K}V, -4\mathcal{K}V\right)\right.$$
$$\left. +\,\frac{4\,\mathcal{K}V\,\mathcal{I}_{11}(\rho,n)}{c_s^2}\,F_1\!\left(\frac{\mathcal{I}_{32}(\rho,n)}{n}, -c_s^2(1+\rho), 2\rho c_s^2; \frac{\mathcal{I}_{53}(\rho,n)}{n}; -2\mathcal{K}V, -4\mathcal{K}V\right)\right], \tag{13}$$

where $\mathcal{I}_{ab}(\rho,n) \equiv \big(n(a\rho-b)+2\rho\big)/(2\rho-1)$ and F_1 is the Appell hypergeometric function [56]. The V appearing in (13) is evaluated at sound-horizon exit (i.e., at N_*).

The complexity of F_1 prevents an exact inversion $V(N)$ in closed form. However, in the small-mixing regime $|\mathcal{K}|V \ll 1$ (enforced by $f > 0$), one can expand and invert perturbatively. Writing $\epsilon \equiv A^{\frac{2\rho c_s^2}{\mathcal{I}_{11}}}\,\mathcal{K}$, $\kappa(\rho,n,N) \equiv \left(C_\rho\,N\,n^{c_s^2}\mathcal{I}_{11}\right)^{\frac{n}{\mathcal{I}_{11}}}$, one finds

$$V \approx \kappa\,A^{\frac{2\rho c_s^2}{\mathcal{I}_{11}}}\left[1 - \frac{2c_s^2 n(\rho-1)}{\mathcal{I}_{32}}\,\kappa\,\epsilon\right.$$
$$+\frac{2c_s^6 n}{{\mathcal{I}_{32}}^2\mathcal{I}_{53}}\Big(4\rho^2(\rho-3) + 2n\rho\big(15+9\rho^2-28\rho\big)$$
$$\left.+\,n^2\big(\rho\,(69+22\rho^2-73\rho)-20\big)\Big)(\kappa\epsilon)^2 + \mathcal{O}(\epsilon^3)\right]. \tag{14}$$

Combining (10) with (14) gives the slow-roll parameters directly as functions of N. To second order in ϵ one obtains

$$\varepsilon_H \approx \frac{n}{2\,\mathcal{I}_{11}\,N}\Bigg[1+\frac{2c_s^4}{\mathcal{I}_{32}}\,\mathcal{I}_{21}\,\kappa\,\epsilon-\frac{4c_s^6}{\mathcal{I}_{32}{}^2\mathcal{I}_{53}}\Big(8\rho^3+24n\rho^2(2\rho-1)+2n^2\rho\big(12+\rho(47\rho-50)\big) + n^3\big(\rho(48+58\rho^2-95\rho)-7\big)\Big)\kappa^2\epsilon^2+\mathcal{O}(\epsilon^3)\Bigg], \quad (15)$$

$$\eta_H = -\frac{1}{\varepsilon_H}\frac{d\varepsilon_H}{dN} \approx \frac{1}{N}\Bigg[1-\frac{2nc_s^4}{\mathcal{I}_{32}\mathcal{I}_{11}}\,\mathcal{I}_{21}\,\kappa\,\epsilon+\frac{4nc_s^6}{\mathcal{I}_{32}{}^2\mathcal{I}_{53}\mathcal{I}_{11}}\Big(n^2\rho(62+113n)-17n^3-2n\rho^2(34+3n(42+37n)) + 4\rho^3(1+2n)(6+n(21+17n))\Big)\kappa^2\epsilon^2+\mathcal{O}(\epsilon^3)\Bigg]. \quad (16)$$

For k–essence the scalar and tensor spectra at sound-horizon exit ($c_s k = aH$) read

$$\mathcal{P}_\mathcal{R} \simeq \left.\frac{H^2}{8\pi^2\,\varepsilon_H\,c_s}\right|_{c_s k=aH}, \qquad \mathcal{P}_t = \left.\frac{2H^2}{\pi^2}\right|_{k=aH}. \quad (17)$$

To first order in slow roll (so that $d\ln k \simeq -dN$) it is standard to define

$$r \equiv \frac{\mathcal{P}_t}{\mathcal{P}_\mathcal{R}} = 16\,\varepsilon_H\,c_s,$$
$$n_s-1 \equiv \frac{d\ln\mathcal{P}_\mathcal{R}}{d\ln k} = -\frac{d\ln\mathcal{P}_\mathcal{R}}{dN} = -2\varepsilon_H-\eta_H-s, \quad (18)$$

with $s \equiv \dot{c}_s/(Hc_s) = 0$ for (1). Using (15) yields the analytic estimate

$$n_s-1 = -\Big(1+\frac{n}{\mathcal{I}_{11}}\Big)\frac{1}{N}\Bigg[1+\frac{4nc_s^6}{\mathcal{I}_{32}{}^2\mathcal{I}_{53}}\Big(8\rho^2+2n\rho(15\rho-7) + n^2\big(5+26\rho^2-25\rho\big)\Big)\kappa^2\epsilon^2+\mathcal{O}(\epsilon^3)\Bigg], \quad (19)$$

which smoothly reproduces the separable non-canonical result [51] in the $\epsilon\to 0$ limit. From (18) and (15), $r(N)$ follows immediately. For $\mathcal{K}<0$ (so that $2f-1<1$ for $V>0$), the ϵ–corrections typically reduce both n_s and r relative to the separable case, moving predictions toward the current ACT–preferred region.

IV. RESULTS

In this section we confront the analytic formulae derived in Secs. II–III with exact background integrations, and interpret them in light of recent constraints on the inflationary parameters—chiefly n_s and r—from ACT in combination with Planck, BK18, and BAO (P–ACT–LB) [8, 9]. Throughout, we evaluate observables at sound-horizon exit ($c_s k = aH$). For each potential the normalization A is fixed by matching the scalar amplitude at the CMB pivot, $\mathcal{P}_\mathcal{R}(k_*) \simeq 2.1\times10^{-9}$ at $k_* = 0.05\,\mathrm{Mpc}^{-1}$. Once A is fixed, we scan the small-mixing parameter ϵ_mix (which coincides with ϵ defined in Sec. III):

$$\epsilon_\mathrm{mix} \equiv A^{\frac{2\rho c_s^2}{\mathcal{I}_{11}}}\,\mathcal{K},$$

which effectively corresponds to scanning the coupling $\mathcal{K}$ at fixed scalar amplitude. The e-fold variable N counts the number of e-folds remaining to the end of inflation, $N=\int_t^{t_e}H\,dt$, so that $N_*\in[50,70]$ brackets the usual reheating uncertainty.

TABLE I. Numerical (subscript N; exact background integration) vs. analytic (subscript A; expansion from Eqs. (15), (18), (19)) predictions for n_s and r at sound-horizon exit for two benchmarks: Model I ($\rho=10$, $n=2$, $N_*=70$) and Model II ($\rho=2$, $n=\frac{2}{3}$, $N_*=60$). The agreement is better than 0.2% for n_s and at the few-percent level for r across the scanned ϵ_mix range.

Model	$\lvert\epsilon_\mathrm{mix}\rvert$	Numerical $n_{s,N}$	Numerical r_N	Analytic $n_{s,A}$	Analytic r_A
I, $\rho=10$, $n=2$, $N_*=70$	0.0001	0.9714	0.0247	0.9713	0.0248
	0.0002	0.9707	0.0231	0.9707	0.0232
	0.0003	0.9691	0.0210	0.9695	0.0211
	0.0004	0.9659	0.0184	0.9655	0.0184
	0.0005	0.9575	0.0148	0.9576	0.0149
II, $\rho=2$, $n=2/3$, $N_*=60$	0.010	0.9755	0.0273	0.9755	0.0271
	0.015	0.9739	0.0231	0.9741	0.0230
	0.020	0.9701	0.0179	0.9712	0.0177
	0.025	0.9578	0.0110	0.9577	0.0107

We compare the analytic predictions from Eqs. (15), (18) and (19) with exact numerical results

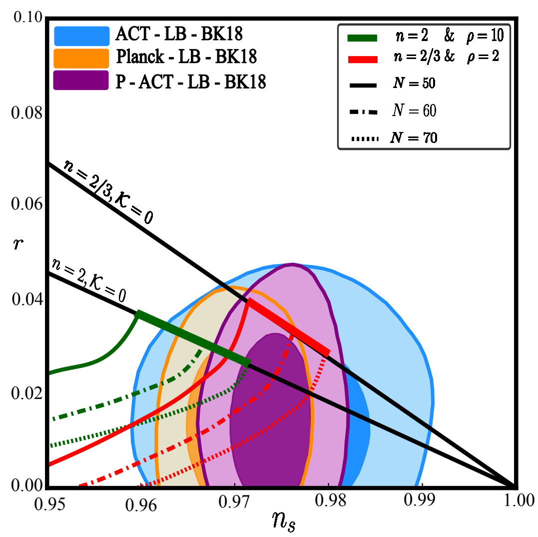

FIG. 1. Predictions in the (n_s, r) plane from Eqs. (15), (18) and (19). Curves correspond to varying $\epsilon_{\rm mix}$ at fixed (ρ, n, N_*); contours combine ACT with Planck 2018, BK18 and BAO (P–ACT–LB).

obtained by solving Eqs. (3) and (4) for $\{\phi(N), H(N)\}$.[2] We denote the mixing expansion parameter by $\epsilon_{\rm mix}$ to avoid confusion with the Hubble slow-roll parameter ε_H.

The agreement in Table I is excellent: typical (maximal) fractional differences are $\lesssim 3\times10^{-4}$ ($\sim 1.1\times10^{-3}$) for n_s and $\sim 0.8\%$ ($\sim 2.7\%$) for r, validating the $\mathcal{O}(\epsilon^2_{\rm mix})$ expansion. For fixed (ρ, n, N_*), dialing $\mathcal{K}<0$—and thus $2f-1<1$ for $V>0$—systematically shifts both n_s and r downward relative to the separable limit, as anticipated analytically. On the data side, the ACT+Planck+BAO combination (P–ACT–LB) prefers $n_s = 0.9743 \pm 0.0034$ with $r < 0.038$ (95% CL) [8, 9]; several entries in Table I fall squarely in this window. The model flow in the (n_s, r) plane obtained from Eqs. (15) and (19), with observational contours overlaid, is shown in Fig. 1.

A broader view of parameter dependence is provided in Fig. 2, which displays the allowed region in $(\epsilon_{\rm mix}, \rho, N_*)$ for $n=2$ and $n=2/3$. Increasing ρ (thereby decreasing c_s) and/or increasing $|\mathcal{K}|$ lowers r at fixed N_*, while n_s is chiefly controlled by N_* and only gently shifted by $\epsilon_{\rm mix}$. In particular, within the scans shown we find that agreement with P–ACT–LB typically requires

$$\text{for } V = A\phi^2 : N_* \gtrsim 70, \quad \rho \gtrsim 10, \quad -6.2\times10^{-4} < \epsilon_{\rm mix} \le 0,$$

$$\text{for } V = A\phi^{2/3} : N_* \gtrsim 50, \quad \rho \gtrsim 1, \quad -3.19\times10^{-2} < \epsilon_{\rm mix} \le 0\ .$$

Two-dimensional slices at fixed N_* are shown in Fig. 3.

Finally, we assess robustness within the same narrative flow. Varying N_* in the canonical range $[50, 70]$ shifts n_s roughly as $\Delta n_s \simeq (1 + n/\mathcal{I}_{11})\,\Delta N_*/N_*^2$, while r scales as $1/N_*$ at leading order; the qualitative impact of the non-separable mixing is unchanged across this interval. Because $c_s^2 = 1/(2\rho-1)$ is constant in our class, the equilateral-type non-Gaussianity scales as $f_{\rm NL}^{\rm equil} \sim \mathcal{O}(c_s^{-2}-1)$ with an $\mathcal{O}(1)$ coefficient set by the cubic couplings of $P(X,\phi)$ [50]. For the benchmarks displayed ($\rho=2$ and $\rho=10$) this corresponds to amplitudes $\mathcal{O}(1\text{–}10)$, comfortably consistent with current bounds. All parameter points in the figures and table satisfy $f(\phi)>0$ and $\rho>1/2$ (no ghosts, $c_s^2>0$), and respect the hard upper bound $V < 1/(2|\mathcal{K}|)$ derived in Sec. II. In short, the non-separable mixing controlled by $\mathcal{K}<0$ systematically lowers both n_s and r relative to the separable non-canonical limit for the monomials tested, enabling otherwise marginal potentials to fit the P–ACT–LB contours while remaining theoretically healthy in the slow-roll regime.

V. CONCLUSION

We studied a non-separable subset of k-essence in which the kinetic and potential sectors interact through an $X^\rho V(\phi)$ coupling implemented via a potential-dependent prefactor $f(\phi) = 1 + 2\mathcal{K}V$. In slow roll this structure modifies the Hubble flow in a controlled way and shifts the inflationary predictions relative to the separable non-canonical template. For monomial potentials $V = A\phi^n$ (with $n=2$ and $n=2/3$ as representative cases) we derived closed analytic expressions for $n_s(N_*)$ and $r(N_*)$ to $\mathcal{O}(\epsilon^2_{\rm mix})$, with $\epsilon_{\rm mix} \propto \mathcal{K}$, and verified them against exact background integrations. The analytic and numerical predictions agree at the sub-per-mille level for n_s and at the percent level for r, validating the small-mixing expansion. Throughout, the class has constant sound speed $c_s^2 = 1/(2\rho-1)$ and satisfies the standard health conditions provided $f(\phi)>0$, $\rho>\frac{1}{2}$, and $V < 1/(2|\mathcal{K}|)$ (the positivity bound from $f>0$).

A robust qualitative outcome is that for $\mathcal{K}<0$ (hence $2f-1<1$ along the trajectory) the non-separable mixing systematically lowers both n_s and r at fixed N_*, moving otherwise marginal monomials toward the region favored by recent ACT+Planck+BK18+BAO constraints (P–ACT–LB). Our parameter scans illustrate viable domains without performing a likelihood fit, and they clarify the roles of N_* (primarily setting n_s), ρ (via c_s), and

[2] In the numerics N decreases to zero at the end of inflation. For each parameter point we verify $f(\phi)>0$ and $\rho>1/2$ (so $c_s^2 = 1/(2\rho-1)>0$), and we enforce the positivity bound $|\mathcal{K}|V < \frac{1}{2}$, equivalent to $f = 1+2\mathcal{K}V>0$.

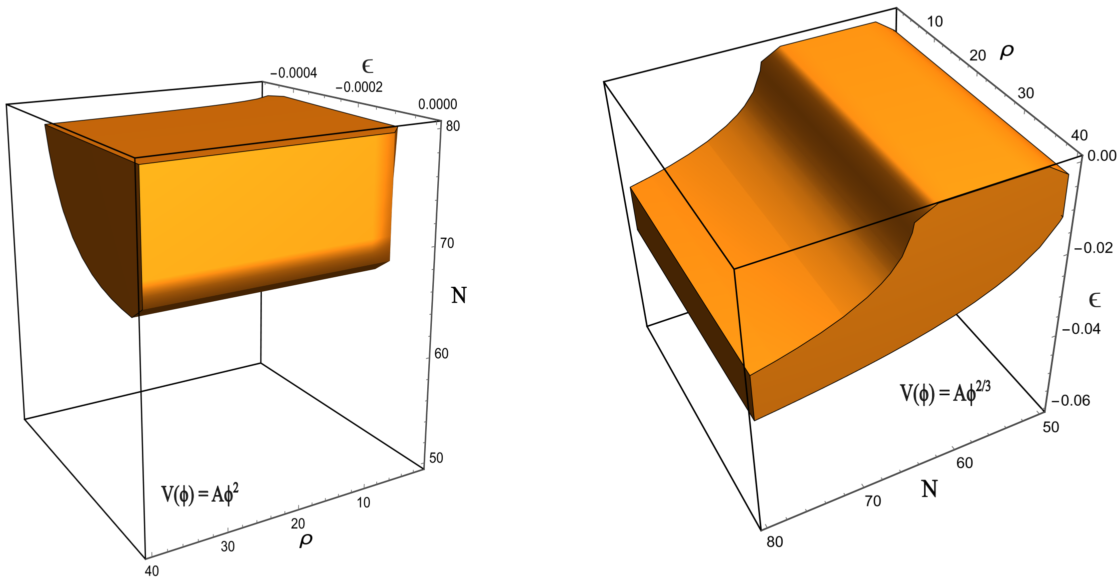

FIG. 2. Allowed region in $(\epsilon_{\rm mix}, \rho, N_*)$ for $n = 2$ (top) and $n = 2/3$ (bottom). Shaded points satisfy the P–ACT–LB constraints on (n_s, r). All shown points also obey $f > 0$ and $|\mathcal{K}|V < \frac{1}{2}$.

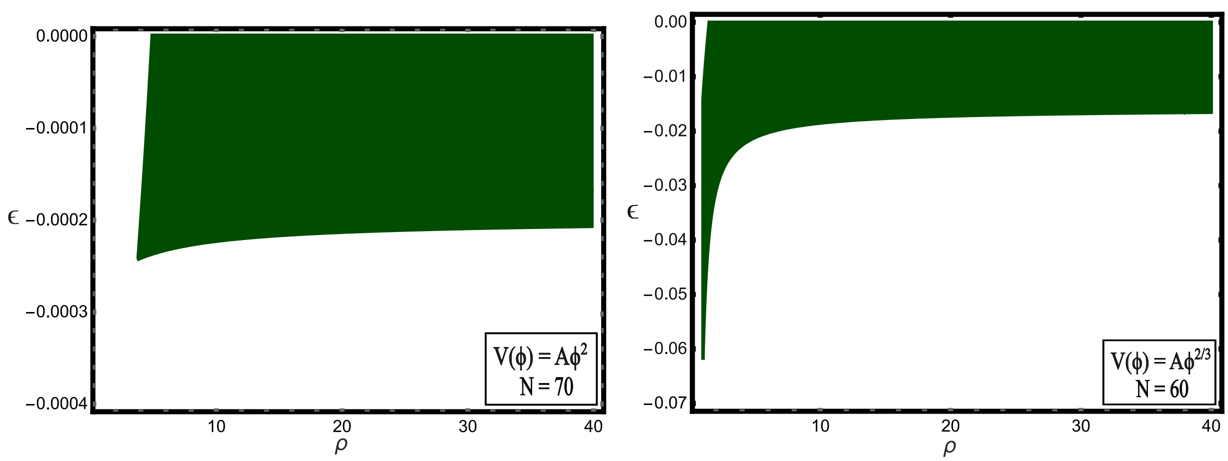

FIG. 3. Slices of Fig. 2 showing the allowed $(\epsilon_{\rm mix}, \rho)$ region for fixed N_* ($N_* = 70$ for $n = 2$ and $N_* = 60$ for $n = 2/3$). Shaded areas lie inside the P–ACT–LB contour.

the mixing strength $\epsilon_{\rm mix}$ (tuning both observables). Because c_s is constant, the leading equilateral bispectrum scales as $\mathcal{O}(c_s^{-2} - 1)$ with an $\mathcal{O}(1)$ coefficient set by the cubic couplings of $P(X, \phi)$; for the benchmarks considered, this implies amplitudes comfortably consistent with current bounds.

A natural continuation is a full statistical confrontation with the P–ACT–LB likelihood (and upcoming CMB-S4/Simons Observatory data), a dedicated bispectrum analysis, and an exploration of broader potentials (e.g., $V = V_0 e^{-\alpha\phi^n}$, $n > 1$) and UV completions that generate the $X^\rho V(\phi)$ interaction. Possible connections to late-Universe tensions (e.g., H_0, S_8) lie outside the scope of the present inflationary study but motivate complementary work in related XV scenarios.

ACKNOWLEDGMENTS

Ö.A. acknowledges the support of the Turkish Academy of Sciences in the scheme of the Outstanding Young Scientist Award (TÜBA-GEBİP). MS is supported by the Science and Engineering Research Board (SERB), DST, Government of India under the Grant

Agreement number CRG/2022/004120 (Core Research Grant). MS is also partially supported by the Ministry of Education and Science of the Republic of Kazakhstan, Grant No. 0118RK00935.

---

[1] A. H. Guth, Inflationary universe: A possible solution to the horizon and flatness problems, Physical Review D **23**, 347 (1981).

[2] A. D. Linde, A new inflationary universe scenario: A possible solution of the problem of cosmological series?, Physics Letters B **108**, 389 (1982).

[3] A. A. Starobinsky, A new type of isotropic cosmological models without singularity, Physics Letters B **91**, 99 (1980).

[4] V. F. Mukhanov and G. V. Chibisov, Quantum fluctuations and a nonsingular universe, JETP Letters **33**, 532 (1981), original English translation of the Russian article.

[5] A. Albrecht and P. J. Steinhardt, Cosmology for grand unified theories with radiatively induced symmetry breaking, Physical Review Letters **48**, 1220 (1982).

[6] G. Hinshaw *et al.*, Nine-year wilkinson microwave anisotropy probe (wmap) observations: Cosmological parameter results, Astrophysical Journal Supplement Series **208**, 19 (2013), wMAP Collaboration.

[7] Y. Akrami *et al.* (Planck), Planck 2018 results. X. Constraints on inflation, Astron. Astrophys. **641**, A10 (2020), arXiv:1807.06211 [astro-ph.CO].

[8] T. Louis *et al.* (ACT), The Atacama Cosmology Telescope: DR6 Power Spectra, Likelihoods and ΛCDM Parameters (2025), arXiv:2503.14452 [astro-ph.CO].

[9] E. Calabrese *et al.* (ACT), The Atacama Cosmology Telescope: DR6 Constraints on Extended Cosmological Models (2025), arXiv:2503.14454 [astro-ph.CO].

[10] L. Balkenhol, S.-G. Collaboration, *et al.*, Measurement of... (provide exact title if known), Physical Review D **108**, 023510 (2023).

[11] J. Ellis, M. A. G. García, N. Nagata, D. V. Nanopoulos, and K. A. Olive, Deformations of Starobinsky Inflation in No-Scale SU(5) and SO(10) GUTs (2025), arXiv:2508.13279 [hep-ph].

[12] I. Antoniadis, J. Ellis, W. Ke, D. V. Nanopoulos, and K. A. Olive, How accidental was inflation?, arXiv (2025), arXiv:2504.12283, arXiv:2504.12283 [hep-ph].

[13] I. D. Gialamas, T. Katsoulas, and K. Tamvakis, Keeping the relation between the starobinsky model and no-scale supergravity active, arXiv (2025), arXiv:2505.03608, arXiv:2505.03608 [hep-ph].

[14] A. Addazi, Y. Aldabergenov, and S. Ketov, Curvature corrections to starobinsky inflation can explain the act results, arXiv (2025), arXiv:2505.10305, arXiv:2505.10305 [hep-ph].

[15] A. M. Yogesh, Q. Wu, and T. Zhu, Starobinsky-like inflation and egb gravity in the light of act, arXiv (2025), arXiv:2505.05363, arXiv:2505.05363 [hep-ph].

[16] M. R. Haque, S. Pal, and D. Paul, Improved predictions on higgs-starobinsky inflation and reheating with act dr6 and primordial gravitational waves, arXiv (2025), arXiv:2505.04615, arXiv:2505.04615 [hep-ph].

[17] M. R. Haque, S. Pal, and D. Paul, ACT DR6 Insights on the Inflationary Attractor models and Reheating (2025), arXiv:2505.01517 [astro-ph.CO].

[18] M. Drees and Y. Xu, Refined predictions for starobinsky inflation and post-inflationary constraints in light of act, Phys. Lett. B **867**, 139612 (2025), arXiv:2504.20757, arXiv:2504.20757 [hep-ph].

[19] R. Kallosh, A. Linde, and D. Roest, A simple scenario for the last act, arXiv (2025), arXiv:2503.21030, arXiv:2503.21030 [hep-th].

[20] S. Aoki, H. Otsuka, and R. Yanagita, Higgs-modular inflation, arXiv (2025), arXiv:2504.01622, arXiv:2504.01622 [hep-th].

[21] R. Mondal, S. Mondal, and A. Chakraborty, Constraining reheating temperature, inflaton-sm coupling and dark matter mass in light of act dr6 observations, arXiv (2025), arXiv:2505.13387, arXiv:2505.13387 [hep-ph].

[22] L. Liu, Z. Yi, and Y. Gong, Reconciling higgs inflation with act observations through reheating, arXiv (2025), arXiv:2505.02407, arXiv:2505.02407 [hep-ph].

[23] S. Maity, Act-ing on inflation: Implications of non-bunch-davies initial condition and reheating on single-field slow-roll models, arXiv (2025), arXiv:2505.10534, arXiv:2505.10534 [hep-th].

[24] Q. Gao, Y. Gong, Z. Yi, and F. Zhang, Non-minimal coupling in light of act, arXiv (2025), arXiv:2504.15218, arXiv:2504.15218 [hep-ph].

[25] C. Dioguardi, A. J. Iovino, and A. Racioppi, Fractional attractors in light of the latest act observations, arXiv (2025), arXiv:2504.02809, arXiv:2504.02809 [hep-ph].

[26] J. McDonald, Higgs inflation with vector-like quark stabilisation and the act spectral index, arXiv (2025), arXiv:2505.07488, arXiv:2505.07488 [hep-ph].

[27] W. Yin, Higgs-like inflation under activated mass, arXiv (2025), arXiv:2505.03004, arXiv:2505.03004 [hep-ph].

[28] Z. Yi, X. Wang, Q. Gao, and Y. Gong, Potential reconstruction from act observations leading to polynomial α-attractor, arXiv (2025), arXiv:2505.10268, arXiv:2505.10268 [hep-ph].

[29] Z. Peng, Z. Chen, and L. Liu, The polynomial potential inflation in light of act observations, arXiv (2025), arXiv:2505.12816, arXiv:2505.12816 [hep-ph].

[30] M. He, M. Hong, and K. Mukaida, Increase of ns in regularized 7-kinetically modified palatini inflation meets act data: pole inflation & einstein-cartan gravity, arXiv (2025), arXiv:2504.16069, arXiv:2504.16069 [hep-ph].

[31] W. J. Wolf, Inflationary attractors and radiative corrections in light of act, arXiv (2025), arXiv:2506.12436, arXiv:2506.12436 [hep-ph].

[32] A. Berera, S. Brahma, Z. Qiu, R. O. Ramos, and G. S. Rodrigues, The early universe is act-ing warm, Phys. Rev. D **111**, 123527 (2025), arXiv:2504.02655, arXiv:2504.02655 [hep-ph].

[33] C. Pallis, Kinetically modified Palatini inflation meets ACT data, Phys. Lett. B **868**, 139739 (2025), arXiv:2505.23243 [hep-ph].

[34] S. D. Odintsov and T. Paul, ACT inflation and its influence on reheating era in Einstein-Gauss-Bonnet gravity, Phys. Lett. B **870**, 139930 (2025), arXiv:2508.11377 [gr-qc].

[35] Y. Zhu, Q. Gao, Y. Gong, and Z. Yi, Inflationary Models with Gauss-Bonnet Coupling in Light of ACT Observations (2025), arXiv:2508.09707 [astro-ph.CO].

[36] S. V. Ketov, E. O. Pozdeeva, and S. Y. Vernov, Inflation in $F(R)$ gravity models revisited after ACT (2025), arXiv:2508.08927 [gr-qc].

[37] M. Zahoor, S. Khan, and I. A. Bhat, Reconciling fractional power potential and EGB gravity in the light of ACT, JHEAp **49**, 100458 (2026), arXiv:2507.18684 [astro-ph.CO].

[38] D. Chakraborty and S. Das, Behaviour of α-attractors in warm inflation, arXiv preprint (2025), arXiv:2506.08489, 2506.08489.

[39] J. Han, H. M. Lee, and J. H. Song, Higgs pole inflation with loop corrections in light of act results, arXiv preprint (2025), arXiv:2506.21189, 2506.21189.

[40] Q. Gao, Y. Qian, Y. Gong, and Z. Yi, Observational constraints on inflationary models with non-minimally derivative coupling by act, arXiv preprint (2025), arXiv:2506.18456, 2506.18456.

[41] S. Choudhury, B. Gulnur, S. K. Singh, and K. Yerzanov, What new physics can we extract from inflation using the act dr6 and desi dr2 observations?, arXiv preprint (2025), arXiv:2506.15407, 2506.15407.

[42] Z. Yi, X. Wang, Q. Gao, and Y. Gong, Potential reconstruction from act observations leading to polynomial α-attractor, arXiv preprint (2025), arXiv:2505.10268, 2505.10268.

[43] M. He, M. Hong, and K. Mukaida, Increase of n_s in regularized pole inflation & einstein-cartan gravity, arXiv preprint (2025), arXiv:2504.16069, 2504.16069.

[44] H. Heidarian, M. Solbi, S. Heydari, and K. Karami, α-attractor inflation modified by GUP in light of ACT observations, Phys. Lett. B **869**, 139833 (2025), arXiv:2506.10547 [astro-ph.CO].

[45] V. K. Oikonomou, String Corrected Scalar Field Inflation Compatible with the ACT Data (2025), arXiv:2508.19196 [gr-qc].

[46] J. Yuennan, P. Koad, F. Atamurotov, and P. Channuie, Quantum-Corrected ϕ^4 Inflation in Light of ACT Observations (2025), arXiv:2508.17263 [astro-ph.CO].

[47] V. K. Oikonomou, Strong Gravity Effects on $\mathcal{R}^2$-corrected Single Scalar Field Inflation and Compatibility with the ACT Data (2025), arXiv:2508.17363 [gr-qc].

[48] S. D. Odintsov and V. K. Oikonomou, Confronting Rainbow-deformed $f(R)$ Gravity with the ACT Data (2025), arXiv:2508.17358 [gr-qc].

[49] C. Armendariz-Picon, T. Damour, and V. F. Mukhanov, k - inflation, Phys. Lett. B **458**, 209 (1999), arXiv:hep-th/9904075.

[50] X. Chen, M.-x. Huang, S. Kachru, and G. Shiu, Observational signatures and non-gaussianities of general single-field inflation, Journal of Cosmology and Astroparticle Physics **2007** (01), 002–002.

[51] S. Li and A. R. Liddle, Observational constraints on k-inflation models, Journal of Cosmology and Astroparticle Physics **2012** (10), 011–011.

[52] C. Cheung, P. Creminelli, A. L. Fitzpatrick, J. Kaplan, and L. Senatore, The Effective Field Theory of Inflation, JHEP **03**, 014, arXiv:0709.0293 [hep-th].

[53] A. Achucarro, J.-O. Gong, S. Hardeman, G. A. Palma, and S. P. Patil, Mass hierarchies and non-decoupling in multi-scalar field dynamics, Phys. Rev. D **84**, 043502 (2011), arXiv:1005.3848 [hep-th].

[54] A. Achucarro, S. Mooij, P. Ortiz, and M. Postma, Sgoldstino inflation, JCAP **08**, 013, arXiv:1203.1907 [hep-th].

[55] S. A. Hosseini Mansoori and H. Moshafi, Alleviating H $_0$ and S $_8$ Tensions Simultaneously in K-essence Cosmology, Astrophys. J. **975**, 275 (2024), arXiv:2405.05843 [astro-ph.CO].

[56] E. T. Whittaker and G. N. Watson, *A Course in Modern Analysis*, 4th ed. (Cambridge University Press, Cambridge, England, 1990).